

AD A091859

DDC FILE COPY

UNCLASSIFIED  
SECURITY CLASS. CATION OF THIS PAGE (When Data Entered)

LEVEL

REPORT DOCUMENTATION PAGE		READ INSTRUCTIONS BEFORE COMPLETING FORM
1. REPORT NUMBER (18) 15042-4-MS	2. GOVT ACCESSION NO. AD-A091859	3. RECIPIENT'S CATALOG NUMBER
4. TITLE (and Subtitle) Computer Simulations for the Microscopic Mechanism of Hot Gas Erosion		5. TYPE OF REPORT & PERIOD COVERED Final Report 1 Sep 77 - 31 Aug 80
6. AUTHOR(s) (10) Bruce C. Garrett		7. PERFORMING ORG. REPORT NUMBER
8. PERFORMING ORGANIZATION NAME AND ADDRESS Battelle Columbus Laboratories Columbus, OH 43201		9. CONTRACT OR GRANT NUMBER(s) (15) DAAG29-77-C-0047
10. CONTROLLING OFFICE NAME AND ADDRESS U. S. Army Research Office Post Office Box 12211 Research Triangle Park, NC 27709		11. REPORT DATE (11) Sep 80
12. MONITORING AGENCY NAME & ADDRESS (if different from Controlling Office) (12) 48		13. NUMBER OF PAGES 40
		14. SECURITY CLASS. (of this report) Unclassified
		15a. DECLASSIFICATION/DOWNGRADING SCHEDULE
16. DISTRIBUTION STATEMENT (of this Report) Approved for public release; distribution unlimited.		
17. DISTRIBUTION STATEMENT (of the abstract entered in Block 20, if different from Report) NA		
18. SUPPLEMENTARY NOTES The view, opinions, and/or findings contained in this report are those of the author(s) and should not be construed as an official Department of the Army position, policy, or decision, unless so designated by other documentation.		
19. KEY WORDS (Continue on reverse side if necessary and identify by block number) gases surface properties metals chemical reactions computerized simulation erosion		
20. ABSTRACT (Continue on reverse side if necessary and identify by block number) A systematic technique for obtaining physical reasonable models of gas-surface interaction potentials was employed. A general computer model has been developed to provide realistic, interaction potentials for chemical reactions of gas species on a variety of surface structures. In order to better understand the model interaction potentials a computer program was developed to help probe and characterize the potential energy hypersurfaces. This enabled critical configurations such as equilibrium geometries and saddle points to be		

DTIC  
ELECTED  
NOV 7 1980  
C

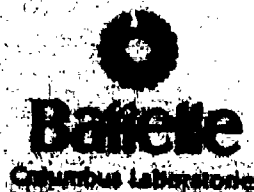
DD FORM 1 JAN 71 1473 EDITION OF 1 NOV 65 IS OBSOLETE

UNCLASSIFIED

SECURITY CLASSIFICATION OF THIS PAGE (When Data Entered)

AD A091859

DOC FILE COPY



# Report

8011 03 097

Unclassified

SECURITY CLASSIFICATION OF THIS PAGE(When Data Entered)

15042 4-MS

20. ABSTRACT CONTINUED

located; the program also provided minimum energy pathways for reactions occurring on the metal surfaces. Classical trajectory studies were carried out for models of direct chemical reaction of gas phase species with surfaces and for atomic recombination reactions occurring on the surfaces. The atomic recombination studies dealt with hydrogen and nitrogen atom recombination on Fe and Ta surfaces. These studies showed that the heat input into the surface from the atomic recombination reaction can be a significant fraction of the total energy of the heat release of the process.

Accession For

NTIS GRA&I	
DTIC TAB	
Unannounced	
Justification	
By	
Distribution /	
Availability Codes	
Dist	

**R**

Unclassified

SECURITY CLASSIFICATION OF THIS PAGE(When Data Entered)

FINAL REPORT

on

Contract # DAAG29-77-C-0047

COMPUTER SIMULATIONS FOR THE MICROSCOPIC  
MECHANISM OF HOT GAS EROSION

to

U. S. Army Research Office

September 30, 1980

Prepared by

Bruce C. Garrett

BATTELLE  
Columbus Laboratories  
505 King Avenue  
Columbus, Ohio 43201

## TABLE OF CONTENTS

	<u>Page</u>
I. PROJECT GOALS. . . . .	1
II. PROJECT ACCOMPLISHMENTS. . . . .	3
A. Summary . . . . .	3
B. Details . . . . .	3
C. Publications Resulting from this Project. . . . .	5
D. Scientific Personnel Supported on this Project. . . . .	5
III. TECHNICAL DISCUSSION. . . . .	6
A. Modeling of the Potential Energy Surface. . . . .	6
B. Classical Trajectory Methods. . . . .	12
REFERENCES . . . . .	18

# LIST OF TABLES

	<u>Page</u>
TABLE I. ATOM-ATOM MORSE PARAMETERS AND LATTICE PARAMETERS FOR THREE METAL SURFACES . . . . .	19
TABLE II. LATTICE POTENTIAL PARAMETERS FOR FIVE SURFACES OF Fe . . . . .	19
TABLE III. LATTICE POTENTIAL PARAMETERS FOR FIVE SURFACES OF Ta . . . . .	20
TABLE IV. LATTICE POTENTIAL PARAMETER FOR FIVE SURFACES OF Cr . . . . .	20
TABLE V. ATOM-ATOM MORSE PARAMETERS FOR GAS PHASE DIATOMICS . . . . .	21
TABLE VI. ATOM-ATOM MORSE PARAMETERS FOR GAS-ATOM INTERACTIONS WITH SEMI-INFINITE SURFACES . . . . .	21
TABLE VII. HYDROGEN ADSORPTION ON SEMI-INFINITE SURFACES OF Fe . . . . .	22
TABLE VIII. HYDROGEN ADSORPTION ON SEMI-INFINITE SURFACES OF Ta . . . . .	22
TABLE IX. HYDROGEN ADSORPTION ON SEMI-INFINITE SURFACES OF Cr . . . . .	23
TABLE X. NITROGEN ADSORPTION ON SEMI-INFINITE SURFACES OF Fe . . . . .	24
TABLE XI. NITROGEN ADSORPTION ON SEMI-INFINITE SURFACES OF Ta . . . . .	25
TABLE XII. NITROGEN ADSORPTION ON SEMI-INFINITE SURFACES OF Cr . . . . .	26
TABLE XIII. Fe-Fe MORSE POTENTIAL PARAMETERS FOR A FINITE CLUSTER OF Fe ATOMS . . . . .	27
TABLE XIV. ATOM-ATOM MORSE PARAMETERS FOR HYDROGEN ADSORPTION ON FINITE Fe CLUSTERS . . . . .	28
TABLE XV. ATOM-ATOM MORSE PARAMETERS FOR HYDROGEN ADSORPTION ON FINITE Ta CLUSTERS . . . . .	28

LIST OF TABLES  
(Continued)

	<u>Pages</u>
TABLE XVI. ATOM-ATOM MORSE PARAMETER FOR HYDROGEN ADSORPTION ON FINITE Cr CLUSTERS. . . . .	29
TABLE XVII. ATOM-ATOM MORSE PARAMETERS FOR NITROGEN ADSORPTION ON FINITE Fe CLUSTERS . . . . .	30
TABLE XVIII. ATOM-ATOM MORSE PARAMETERS FOR NITROGEN ADSORPTION ON FINITE Ta CLUSTERS. . . . .	31
TABLE XIX. ATOM-ATOM MORSE PARAMETERS IN NITROGEN ADSORPTION ON FINITE Cr CLUSTERS. . . . .	32
TABLE XX. ENERGETICS OF ATOMIC RECOMBINATION ON METAL SURFACES . . . . .	33
TABLE XXI. TRAJECTORY RESULTS FOR ATOM RECOMBINATION ON METAL SURFACES BY A RADEAL MECHANISM. . . . .	34
TABLE XXII. RESULTS OF TRAJECTORY CALCULATIONS FOR NITROGEN ATOM RECOMBINATION ON Fe SURFACES FOR NON-NORMAL INCIDENCE OF THE GAS ATOM . . . . .	36

## I. PROJECT GOALS

An understanding of the mechanisms of the erosion of metal surfaces in hot flowing media is important in assessing methods of lessening the effects of wear and erosion upon the performance of large caliber gun tubes. The overall mechanisms of erosion are extremely complex including hydrodynamic flow, chemical reactions, and direct erosion by macroscopic particles. Recent experimental studies<sup>1</sup> indicate that chemical processes may be important in these mechanisms. In this report we present the results of theoretical studies of the microscopic mechanism of chemical erosion which are aimed at assessing the importance of such processes under the physical conditions found in gun tubes.

We consider two broad possibilities of chemical erosion: (1) chemical heating of the surface causing local melting and subsequent removal of the material by the flowing gas stream, and (2) direct chemical erosion in which gaseous species attack surface atoms forming volatile chemical species leading to removal of the surface atoms. By chemical heating of the surface we mean heat input into the surface from chemical processes occurring near the surface. We therefore exclude simple convective heating from our consideration although it is undoubtedly important in the erosion process.

At least two distinct mechanisms of chemical heating can be discerned: (1) heating from chemisorption and (2) heating from recombination reactions. In the process of forming bonds between gaseous species and the surface, energy can be released into the surface. For example, when  $O_2$  chemisorbs on steel it releases  $4.7 \times 10^3$  kJ/kg-metal.<sup>2</sup> When two reactive species such as free radicals recombine to form a single molecule heat can be released into the surface.<sup>3</sup>



Direct chemical reaction of gaseous species with the surface to form a gas-phase species containing a metal atom is similar to the process of chemisorption heating and the subsequent wipe-off of the metal atom by the flowing gas. In both cases the energy liberated from the formation of a gas-metal bond is used to sever the bonding between the metal atom and the remainder of the surface. The major difference is that in direct chemical erosion the metal atom leaves the surface in a bound complex with the gas atom. In direct chemical erosion a surface atom is removed in a single collision event, whereas, in the heat and wipe-off mechanism many collisions can heat the surface leading to the removal of surface atoms.

In summary, the goals of this project were the investigation of chemical mechanisms of hot gas erosion of metal surfaces using theoretical techniques. In particular, the processes of interest are: (1) chemical heating of metal surfaces and (2) direct chemical erosion of metal surfaces. These studies were carried out for a variety of surface structures including perfect crystal surfaces and also surfaces with defects such as steps, kinks, and adatoms. We investigated the importance of the surface defects in the processes mentioned above.

## II. PROJECT ACCOMPLISHMENTS

### A. Summary.

A systematic technique for obtaining physical reasonable models of gas-surface interaction potentials was employed. A general computer model has been developed to provide realistic, interaction potentials for chemical reactions of gas species on a variety of surface structures.

In order to better understand the model interaction potentials a computer program was developed to help probe and characterize the potential energy hypersurfaces. This enabled critical configurations such as equilibrium geometries and saddle points to be located; the program also provided minimum energy pathways for reactions occurring on the metal surfaces.

Classical trajectory studies were carried out for models of direct chemical reaction of gas phase species with surfaces and for atomic recombination reactions occurring on the surfaces. The atomic recombination studies dealt with hydrogen and nitrogen atom recombination on Fe and Ta surfaces. These studies showed that the heat inputted into the surface from the atomic recombination reaction can be a significant fraction of the total energy of the heat release of the process.

### B. Details.

In this work we studied interactions of atomic and diatomic gas species with surfaces. Of particular interest was the transfer of heat from reacting gas species into the surface. Therefore, the model had to allow for motion of the surface atoms as well as the gas-phase species. Such a model

was developed and has been previously described.<sup>4,5</sup> This model is semiempirical and the parameters of the model were chosen to best reproduce experimental data when it was available. An important feature of this model is its ability to model surfaces with steps, kinks, adatoms, etc. Further details of the surface fitting for particular systems are presented in the technical section.

Direct chemical erosion of metal surfaces can occur if sufficient energy from chemisorption of the gaseous species is transferred into breaking the bond between a metal atom and the rest of the surface. Surface atoms at step-sites, kink-sites, or surface adatoms are bound more weakly to the surface than surface atoms with their full complement of nearest neighbors. Therefore, one might expect that direct chemical erosion of surface atoms at step- or kink-sites may be more favorable than for surface atoms at perfect crystal sites. However, we have run several thousand trajectories on surfaces with various defects - i.e., step, kink, etc. - and have found no evidence of direct chemical erosion.

Studies of recombination heating of the solid by a Langmuir-Hinshelwood mechanism have been previously reported.<sup>6</sup> We report here work in which we have studied in detail recombination occurring by a Rideal mechanism. We have also examined the effects of steps and kinks upon the heating of the surface. A surprising outcome of this study was the relative insensitivity of the heating of the surface upon parameters such as temperature of the solid and incident translational energy of the impinging atom.

C. Publications Resulting From this Project

G. Wolken, Jr., "Model Potential for Reactions with Solid Surfaces:  $H_2 + F_e(001)$ "; J. Chem. Phys. 68, 4338 (1978).

G. D. Purvis and G. Wolken, Jr., "Model Potential for the Interaction of Molecules with Amorphous Surfaces", Chem Phys. Lett., 62, 42 (1979).

D. Scientific Personnel Supported on this Project

The following Battelle staff members were supported by funds from this project:

Bruce C. Garrett  
George D. Purvis, III  
Michael J. Redmon  
George Wolken, Jr.

### III. TECHNICAL DISCUSSION

#### A. Modeling of the Potential Energy Surface.

The model potential used for the interaction of diatomic gas species with solid surfaces is described in Appendix A. The potential  $V_{LEPS}$  is based upon the semiempirical London-Eyring-Polanyi-Sato (LEPS) description of gas-solid bonding.<sup>7</sup> The functional form is given in Equations 5-9 of Appendix A. The parameters which must be specified are the dissociation energy  $D_{PQ}$ , the Morse range parameters  $\alpha_{PQ}$ , the equilibrium geometry  $R_{PQ}$  and the Sato parameter  $\Delta_{PQ}$  for the two body interactions between atoms P and Q. P (and Q) can be A or B, one of the gas atoms, or one of the surface atoms. This model is capable of describing the interaction of a diatomic molecule with a surface of moving atoms - the instantaneous locations of the surface atoms are used in evaluating the potential expression - however, the total potential energy is the sum of  $V_{LEPS}$  and the potential energy  $V_{LAT}$  obtained from displacements of the lattice from its equilibrium geometry. The lattice potential was described by a modified Einstein model in which the potential was given in terms of displacements of the atoms from their individual equilibrium positions in a rigid lattice. Because we were interested in describing situations in which large amounts of energy can be transferred to the surface we used an anharmonic potential, the Morse potential, rather than the usual harmonic Einstein model.<sup>8</sup> In the following we describe how the parameters of this model were determined. In all cases the parameters were calculated so that the models reproduced experimental data when it was available.

Consider first the parameters for the lattice potential

$$V_{LAT} = D_{LAT} [1 - e^{-\alpha_{LAT} d}]^2 - D_{LAT} \quad (1)$$

where  $d$  is the displacement from the equilibrium lattice site location. Girifalco and Weizer<sup>9</sup> used the sum of two-body Morse potential between all surface atoms to describe metal bonding. Using the results of their work we obtained the parameters of the modified Einstein oscillators. From Girifalco and Weizer's work the total potential  $\phi$  felt by one "test atom" in the lattice was obtained by summing over the two-body interactions between the "test atom" and all other atoms in the lattice. The lattice was assumed to be semi-infinite, that is the sums were over lattice positions with  $x$  and  $y$  ranging from  $-\infty$  to  $\infty$  and  $z$  from  $0$  to  $-\infty$ . In practice the sums were done over a sufficient number of lattice sites to insure convergence. The "test atom" was taken to be in the top layer of the lattice; all other atoms in the lower layers were fixed at their equilibrium lattice sites. The lattice constant ( $a$ ) was taken from Girifalco and Weizer<sup>9</sup> when available or from Pearson<sup>10</sup> and we considered only 100 faces of the lattices. The locations of the atoms in the top layer were relaxed from their lattice sites so that the forces on the test atom vanished. A more physical model would also include relaxation of the lower layers, however, since this effect was small for the top layer and decreased for the lattice layers below the surfaces we neglected it for all but the top layer. This determined the equilibrium geometry and therefore the value of the potential at this location was the negative of the energy necessary to remove the atom from the surface.

(This assumes the zero of energy for all the two-body potentials was at infinite separation of the atoms.) This defined  $D_{\text{LAT}}$  and the range parameters  $\alpha_{\text{LAT}}$  was obtained from

$$\alpha_{\text{LAT}} = \left[ \frac{1}{2D_{\text{LAT}}} \frac{\partial^2 \phi}{\partial z^2} \right] \quad (2)$$

evaluated at the equilibrium geometry. The  $z$  direction was taken to be perpendicular to the surface, therefore,  $\alpha_{\text{LAT}}$  was the range parameter for motion normal to the surface. In general, the range parameters for motion in the surface plane will be different than for out of the plane, but we did not take this into account in our model.

Using the sum of pair potentials we assessed the effect of surface defects (steps, kinks, etc.) upon the bonding of the metal atoms to the surface. As surface atoms were removed, the "test atom" became less tightly bound decreasing  $D_{\text{LAT}}$ , and also the equilibrium geometry and range parameters for the test atom changed. We considered five types of surfaces: (1) a regular crystal surface (no defect), (2) a simple step in which all the top layer atoms in the left half of the  $x$ - $y$  plane had been removed, (3) a kink in which all the top layer atoms in all but the upper right quadrant of the  $x$ - $y$  plane had been removed, (4) an adatom next to a simple step, and (5) a lone adatom (removal of all the top surface atoms except for the "test atom.")

In Table I the atom-atom Morse parameters from Girifalco and Weizer's work along with the lattice parameters for Fe, Ta, and Cr surfaces are listed. In Tables II-IV we present our calculated equilibrium

geometries and lattice potential parameters for these five surface defects on Fe, Ta, and Cr surfaces. As the number of nearest neighbors decreased the bonding of the "test atom" also decreased. The sublimation energy at zero temperature and pressure is a weighted average of the dissociation energies for the different surface sites of the lattice, therefore we expected our values of  $D_{LAT}$  for the different surface defects to bracket the experimental sublimation energy. For Fe and Cr the sublimation energies are 97 and 90 kcal/mol, respectively,<sup>11</sup> and for Ta it is estimated from the experimental values of Mo and W to be between 160 and 200 kcal/mol.

We next consider the manner in which the parameters of the gas-surface interaction potential  $V_{LEPS}$  were determined. In the limit that the gas-phase atom A and B are well above the surface,  $V_{LEPS}$  reduces to a Morse function with dissociation energy  $D_{AB}$ , range parameter  $\alpha_{AB}$ , and equilibrium geometry  $R_{AB}$ . These values were fit from experimental values for  $H_2$  and  $N_2$ ,<sup>12</sup> and for FeH we used a theoretical estimate.<sup>13,14</sup> Values of these parameters are listed in Table V.

In the limit that one of the gas-phase atoms A is far removed from the surface and the other B is on the surface, the potential equals the adsorption energy of atom B on the surface. This was obtained by summing the pair potential between the adsorbing atom and all of the surface atoms. The pair potential is a Morse function with dissociation energy  $D_{BS}$ , range parameters  $\alpha_{BS}$ , and equilibrium geometry  $R_{BS}$ , where S denotes a surface atom. Olander<sup>15</sup> has treated the adsorption of hydrogen atoms on Fe and Ta surfaces of infinite lattices without surface defects.



The gas-surface Morse parameters for H on Cr and for N on all three metal surfaces have been estimated.<sup>16</sup> The atom-atom Morse parameters for these systems are presented in Table VI. The location of the adsorbing atom was optimized such that the forces on it vanish. The potential at this location was the negative of the adsorption energy, and we also calculated the frequency of the motion of the adsorbed atom normal to the surface. These values are listed in Tables VII-XII for H on N adsorbing on three of the surface types (no defect, step, and kink) for Fe, Ta, and Cr.

In our dynamical calculations it was impractical to use semi-infinite surfaces, therefore, it was necessary to consider small clusters of metal atoms, 30-46 atoms. In the sum of pairs model, if the number of surface atoms was decreased the bonding of the adsorbed atom also decreased. Therefore, we found it necessary to reoptimize the atom-atom interaction parameters so that the adsorption energy and vibrational frequency of the adsorbed atom would be the same as on the semi-infinite surfaces. This was done by finding the values of  $D_{BS}$ ,  $\alpha_{BS}$ , and  $R_{BS}$  that would simultaneously give the correct equilibrium height above the surface, adsorption energy, and vibrational frequency for the adsorbing atom. These parameters depend upon the size of the cluster. We found that different cluster sizes were needed to properly describe the different dynamical events - direct chemical reaction and recombination heating - and we describe both below.

First consider the direct chemical reaction of a gas atom A with a surface atom to form a gas-phase species in which A is bonded to the metal atom. We treated the metal atom that was attacked as the

species B adsorbed to the surface. The parameters for the two-body potential between B and the other surface atoms was just those given by Girifalco and Weizer<sup>9</sup> for the case of an semi-infinite lattice. In our dynamical calculations we used a cluster of 45 metal atoms plus the atom B to represent the surfaces with no defects. For a surface with no defects, twenty atoms were used in the top layer (a 5 x 5 grid with atoms removed from the corner and the central atom replaced by atom B), 12 in the second layer (a 4 x 4 grid with atoms removed from the corners), 9 in the third layer (a 3 x 3 grid), and 4 in the fourth layer (a 2 x 2 grid). The reoptimized atom-atom Morse parameter for this finite lattice are presented in Table XIII for the five surface defects described above. These parameters should be compared with those in Table I for an estimate of the effect of finite cluster size upon the Morse parameters.

In modeling the direct chemical erosion process we used the Morse parameters for FeH listed in Table V and for H on the Fe surface we used the parameters given in Table XIV. The specification of the interaction potential  $V_{LEPS}$  is completed by selecting the Sato parameters. The Sato parameters were varied to obtain the best qualitatively correct description of the adsorption of H on the Fe surface. We found that for all  $\Delta$ 's equal to zero the adsorption energy on defect free Fe was 50 kcal/mol with an equilibrium height of H above the surface of 3.6  $a_0$ . These numbers compare well with the values in Table VII.

For describing recombination heating we used a cluster size of 30 atoms for the lattice with no surface defect. This cluster had 16 atoms in the top layer (a 4 x 4 grid), 9 atoms in the second layer

(a  $3 \times 3$  grid), 4 atoms in the third layer (a  $2 \times 2$  grid) and finally a single atom in the fourth layer. The reoptimized atom-atom Morse parameters for H and N adsorption on Fe, Ta, and Cr are summarized in Tables XIV-XIX for three types of surfaces - no defect, step, and kink. These should be compared with those in Table VI to see the effect of finite cluster size upon the potential parameters describing adsorption.

The Morse parameters used in  $V_{LEPS}$  can be found in Tables V and XIV-XIX. The specification of the interaction potential is completed by selecting values for the Sato parameters. Because we had no guide for their selection we used the values zero as in previous applications.<sup>5</sup> We performed a detailed study of the interaction potential used for the Rideal recombination of  $H_2$  on Fe. The adsorbed H was placed at a 4-fold equilibrium site  $3.13 a_0$  above the top layer. The second H atom was brought down directly over the adsorbed H and the adsorbed H was allowed to relax to its equilibrium position and a local minimum in the potential was found when the second H was  $4.76 a_0$  above the surface and the adsorbed H was  $2.45 a_0$  above the surface. This local minimum was higher in energy by only 0.4 kcal/mol than desorbed  $H_2$  far removed from the surface. However, there is a 6.3 kcal/mol barrier to this desorption process. The barrier to this process had its maximum when the desorbing atoms were 6.63 and 5.14 kcal/mol above the surface.

#### B. Classical Trajectory Methods.

All of the trajectory calculations performed here were for the general event in which a single atom collided with an adsorbed atom and the desired outcome was a reactive event in which the adsorbed atom and incident gas atom form a new bond and leave the surface. A

sufficiently large cluster of metal atoms was used to give a physically correct description of the interaction potential. Only a small number, generally 4-8, of the surface atoms were allowed to move. The others were fixed at their lattice site locations. A unique trajectory was specified by selection of the initial position and momentum vectors of the moving surface atoms, the adsorbed atom, and the incident atom. It was assumed that the surface and adsorbed atom are at thermal equilibrium characterized by a temperature  $T$ . The momenta for these atoms were selected from a Boltzmann distribution by importance sampling.<sup>17</sup> The positions of these atoms were also selected from a Boltzmann distribution but using Metropolis sampling.<sup>18</sup> The incident atom was started at an arbitrary and large distance above the surface, generally  $10 a_0$ . The incident angle was specified and the  $x, y$  coordinates were chosen so that an undeflected straight line trajectory would hit the surface at  $x_0, y_0$ . The coordinates  $x_0, y_0$  were chosen randomly on a square of length equal to the lattice parameter. The momentum vector was chosen along the incident angle with magnitude equal to the specified initial translation energy of the atom plus any potential attraction it may feel from the surface. This potential term was evaluated by subtracting the value of the total potential with the incident atom at its initial location from the total potential with the incident atom moved infinitely far from the surface.

Direct chemical erosion was modeled only for H incident upon Fe surfaces. In the gas-phase Fe-H is bound by about 60 kcal/mol and Fe is bound to the metal surface by 74-128 kcal/mol depending upon whether the Fe atom is in a smooth face of the lattice or at a surface defect site.

Therefore the process of H pulling a Fe atom off the surface is uphill in energy by 14-68 kcal/mol. The most energetically favorable situation is for an H atom to attack an adatom on the surface. Even in this situation the H atom must have about 14 kcal/mol (0.6 eV) of translational energy to surmount the barrier to form  $\text{FeH(g)}$ . At these relatively high translational energies the light hydrogen atom is moving very rapidly making the prospects of it interacting strongly with a heavy Fe atom very low. From this kinematic argument it is not surprising that no evidence was seen for direct chemical erosion with hydrogen. To further study this problem we extended our model calculations to include collision of heavier incident atoms with more favorable mass ratios with the Fe. The potential was still modeled using the hydrogen parameters, and only the mass of the incident atom was changed so that we could assess whether the nonreactivity of the Fe surface was due to this kinematic effect or a more subtle effect from a combination of the potential surface and structure of the surface. When we increased the mass of the incident atom we still saw no evidence of direct chemical erosion and therefore we believe that this mechanism will contribute negligibly to the hot-gas erosion of Fe surfaces. Tantalum atoms are even more strongly bound to the surface than are Fe atoms and direct chemical reaction with Ta atoms in the surface is energetically less favorable than with Fe surfaces. The surface structure, sublimation energy, and adsorption of hydrogen is very similar for Fe and Cr, and, therefore, the same general conclusion will hold for this surface also.

We have performed detailed studies of recombination heating by a Rideal mechanism for a subset of the gas-surface interactions we have modeled. Hydrogen-atom recombination has been studied on defect free a Fe surface. Nitrogen-atom recombination on Fe surfaces has been studied for surfaces with no defects and surfaces with steps and kinks for the two different sets of N-Fe Morse parameters. Nitrogen-atom recombination on Ta surfaces has been studied for surfaces with no defects and with steps. The atom recombination reactions of all of the systems are exoergetic, that is they release energy; the net exoergicity is the difference between the energy of the new gas-phase diatomic bond that is formed and the adsorption energy of the atom. The values of the exoergicities for the various systems are given in Table XX. We were interested in how much of the exoergicity can be deposited into the surface. Because the nitrogen molecule forms a much stronger bond than the hydrogen molecule, N-atom recombination is a better choice for studying the surface heating. In fact, for hydrogen recombination on Ta surfaces the exoergicity is only 6-10 kcal/mol depending upon the surface structure (i.e., step or kinks, etc.). This is the reason that most of our detailed studies are on N-atom recombination.

Although the recombination process is energetically favorable for all of these systems, for some of the systems there is a more stable intermediate complex - the adsorption of two atoms at different equilibrium sites on the surfaces. This energy will be close to the sum of adsorption for the two atom independent but slightly different because of their interaction which is normally repulsive in our models. In all our

models the diatomic dissociated upon adsorption. We found that for  $H_2$  on Fe and  $N_2$  on Fe using Morse parameter set (2), that two adsorbed atoms were the most favorable geometry. For these systems the reaction probabilities are small on a short time scale, however, given a sufficiently long time the probability increases that the two atoms will recombine and leave the surface. However, this then becomes a Langmuir-Hinshelwood type mechanism which we exclude from our consideration here. Work on this mechanism has been treated earlier.<sup>6</sup>

A summary of our trajectory results are presented in Tables XXI and XXII. As noted above the two systems  $H_2$  on Fe and  $N_2$  on Fe with Morse parameter set 2 show small probabilities for a direct recombination reaction, the primary event to occur is adsorption of the incident atom. The estimate of energy transfer for these systems is crude because of the small number of reactive events, nonetheless, the estimates are that between 10% and 50% of the exoergicity is deposited into the surface. For the other systems the statistics are much better. For  $N_2$  on Fe using the Morse parameter set 1 and for normal incidence upon the surface, the fraction of exoergicity deposited into the surface is about 24-33%, independent of the incident energy, surface temperature, or surface structure. For  $N_2$  on Ta using Morse parameter set 1 the fraction of exoergicity deposited into the surface in the range 5-11% and again it is independent of incident energy, surface temperature, or surface structure. The trajectory results for gas atoms impinging on the surface at an angle, see Table XXII, show a slight enhancement of the fraction of energy transferred to the surface by the results are similar to those from the calculation with normal incidence.

The major conclusion to be drawn from these studies are that (1) atom-recombination heating of the surface can be quite important--up to 40% of the bond energy of  $N_2$  was found to be transferred to the Fe surface and (2) energy transfer to the surface is more facile for Fe than for Ta surfaces. For systems in which the probability of the Rideal mechanism is low recombination can still occur by a Langmiun-Hinshelwood mechanism. For this type of system we expect heating of the surface to be less important since a great deal of the new bond energy is used up in desorption from the surface. Ta is a heavier atom and is more cohesive in a lattice than Fe. The heavy mass and tight bonding of Ta tend to make it less perturbed by the light gas atom and thus it adsorbs less energy. A surprising outcome is that the surface defects had little effect upon either the reaction probability  $P_R$  or the energy transfer. However, this can be viewed as an encouraging results since the simpler models of perfect crystal surfaces with no defects give the right qualitative behavior.



1. A. C. Alkidas, S. O. Morris, and M. Summerfield, J. Spacecraft 13, 461 (1976); E. G. Platt, A. C. Alkidas, R. E. Shrader, and M. Summerfield, J. Heat Transfer 97C, 110 (1975); A. C. Alkidas, S. O. Morris, and M. Summerfield, AD-A020, 537 (October 1975).
2. A. Gany, L. H. Caveny, M. Summerfield, J. Heat Transfer, 100, 531 (1978).
3. B. Halpern and D. Rosner, J. Chem. Soc. Faraday I, 74, 1883 (1978).
4. G. Wolken, Jr. J., Chem. Phys. 68, 4338 (1971).
5. G. D. Purvis and G. Wolken, Jr., Chem. Phys. Lett., 62, 42 (1979).
6. G. D. Purvis, M. J. Redmon, and G. Wolken, Jr. "The Heating of Solids by Atomic Recombination Occurring on the Surface," unpublished.
7. H. S. Johnston, "Gas Phase Reaction Rate Theory," (Ronald, New York, 1966) p. 171-178.
8. R. A. Oman, J. Chem. Phys. 48, 3919 (1968).
9. L. A. Girifalco and V. G. Weizer, Phys. Dev. 114, 687 (1959).
10. W. B. Pearson, "A Handbook of Lattice Spacings and Structures of Metals and Alloy", Vol. 4, (Pergamon Press, New York, 1958).
11. R. Fürth, Proc. Roy. Soc. (London) A183, 87-110 (1944).
12. K. P. Huber and G. Herzberg, "Molecular Spectra and Molecular Structure IV Constants of Diatomic Molecules," (Van Nostrand Reinhold, New York, 1979).
13. J. H. Walker, T.E.H. Walker, and H. P. Kelley, J. Chem. Phys. 57, 2094 (1972).
14. P. R. Scott and W. G. Richards, J. Chem. Phys. 63, 1690 (1975).
15. D. R. Olander, J. Phys. Chem. Solids 32, 2499 (1971).
16. G. Ehrlich, J. Chem. Phys. 31, 1111 (1959).
17. J. M. Hammensley and D. C. Handscomb, "Monte Carlo Methods" (Methuen, London, 1967).
18. J. P. Valleau and S. G. Whittington, in "Statistical Mechanics Part A: Equilibrium Techniques" ed. by B. J. Berne, (Plenum Press, New York, 1977).

TABLE I. ATOM-ATOM MORSE PARAMETERS AND LATTICE PARAMETERS FOR THREE METAL SURFACES

Metal	$D_M^a$ (kcal/mol)	$\alpha_M^b(a_0^{-1})$	$r_M^c(a_0)$	$a^d(a_0)$
Fe	9.63	0.735	5.38	5.42
Ta <sup>e</sup>	21.50	0.731	5.97	6.25
Cr	10.18	0.832	5.20	5.44

<sup>a</sup> Morse dissociation energy.

<sup>b</sup> Morse range parameter.

<sup>c</sup> Morse equilibrium geometry.

<sup>d</sup> Lattice parameter.

<sup>e</sup> These values were estimated from the results for  $M_0$  and  $W$  of Reference 9 (see Reference 15).

TABLE II. LATTICE POTENTIAL PARAMETERS FOR FIVE SURFACES OF Fe

Defect <sup>c</sup>	Equilibrium Geometry <sup>a</sup>			Lattice Potential Parameters <sup>b</sup>	
	$x(a_0)$	$y(a_0)$	$z(a_0)$	$D_{LAT}$ (kcal/mol)	$\alpha_{LAT}(a_0^{-1})$
none	0.0	0.0	0.474	127.9	0.368
step	0.128	0.0	0.482	111.0	0.390
kink	0.128	0.022	0.482	101.1	0.408
adatom-step	0.128	0.0	0.482	91.1	0.429
adatom	0.0	0.0	0.474	73.8	0.473

<sup>a</sup> The equilibrium geometry is given as the displacement from the unrelaxed lattice site. The z-axis is normal to the surface.

<sup>b</sup> See Equation (1).

<sup>c</sup> The defects are discussed in Section III.A.

TABLE III. LATTICE POTENTIAL PARAMETERS FOR FIVE SURFACES OF Ta.

Defect <sup>c</sup>	Equilibrium Geometry <sup>a</sup>			Lattice Potential Parameters <sup>b</sup>	
	x(a <sub>0</sub> )	y(a <sub>0</sub> )	z(a <sub>0</sub> )	D <sub>LAT</sub> (kcal/mol)	$\alpha_{LAT}(a_0^{-1})$
none	0.0	0.0	0.412	245.7	0.364
step	0.174	0.0	0.427	214.9	0.383
kink	0.132	0.132	0.430	188.6	0.401
adatom-kink	0.174	0.0	0.428	172.6	0.423
adatom	0.0	0.0	0.412	140.1	0.464

<sup>a</sup> The equilibrium geometry is given as the displacement from the unrelaxed lattice site. The z-axis is normal to the surface.

<sup>b</sup> See Equation (1).

<sup>c</sup> The defects are discussed in Section III.A.

TABLE IV. LATTICE POTENTIAL PARAMETER FOR FIVE SURFACES OF Cr

Defect <sup>c</sup>	Equilibrium Geometry <sup>a</sup>			Lattice Potential Parameters <sup>b</sup>	
	x(a <sub>0</sub> )	y(a <sub>0</sub> )	z(a <sub>0</sub> )	D <sub>LAT</sub> (kcal/mol)	$\alpha_{LAT}(a_0^{-1})$
none	0.0	0.0	0.353	117.3	0.414
step	0.152	0.0	0.366	102.6	0.436
kink	0.115	0.115	0.368	90.1	0.461
adatom-kink	0.152	0.0	0.366	82.5	0.481
adatom	0.0	0.0	0.353	67.0	0.527

<sup>a</sup> The equilibrium geometry is given as the displacement from the unrelaxed lattice site. The z-axis is normal to the surface.

<sup>b</sup> See Equation (1).

<sup>c</sup> The defects are discussed in Section III.A.

TABLE V. ATOM-ATOM MORSE PARAMETERS FOR GAS PHASE DIATOMICS

AB	Morse Parameters		
	$D_{AB}(\text{kcal/mol})$	$\alpha_{AB}(a_0^{-1})$	$R_{AB}(a_0)$
$H_2^a$	109.0	1.044	1.401
$N_2^a$	228.4	1.42	2.07
$FeH^b$	60.1	0.74	2.82

<sup>a</sup> Reference 12.<sup>b</sup> Estimated from References 13 and 14.TABLE VI. ATOM-ATOM MORSE PARAMETERS FOR GAS-ATOM INTERACTIONS WITH SEMI-INFINITE SURFACES<sup>a</sup>

Metal	Gas Atom B	Morse Parameter Set	Morse Parameters		
			$D_{BS}(\text{kcal/mol})$	$\alpha_{BS}(a_0^{-1})$	$R_{BS}(a_c)$
$Fe^b$	H		4.60	0.488	6.07
$Fe^c$	N	(1)	6.80	0.550	6.75
		(2)	7.55	0.470	6.40
$Ta^b$	H		17.0	0.841	4.69
$Ta^c$	N	(1)	17.0	0.841	4.69
		(2)	15.58	0.580	6.25
$Cr^c$	H	(1)	5.20	0.495	6.05
		(2)	6.72	0.564	6.41
$Cr^c$	N	(1)	7.40	0.545	6.85
		(2)	7.76	0.462	6.56

<sup>a</sup> For those cases with two entries the values presented cover a range of the estimates for the parameters.<sup>b</sup> Reference 15.<sup>c</sup> Estimated.

TABLE VII. HYDROGEN ADSORPTION ON SEMI-INFINITE SURFACES OF Fe.

Defect <sup>b</sup>	Equilibrium Geometry <sup>a</sup>			Adsorption Energy (kcal/mol)	Vibrational Frequency Normal to Surface (cm <sup>-1</sup> )
	x(a <sub>0</sub> )	y(a <sub>0</sub> )	z(a <sub>0</sub> )		
none	2.71	2.71	3.60	66.7	690
step	3.11	2.71	3.78	61.0	694
kink	3.05	3.05	3.87	56.4	688

<sup>a</sup> The origin was located at a lattice site in the top layer of an unrelaxed lattice. The calculations were performed with the top layer of the surface in its relaxed geometry.

<sup>b</sup> The defects are discussed in Section III.A.

TABLE VIII. HYDROGEN ADSORPTION ON SEMI-INFINITE SURFACES OF Ta.

Defect <sup>b</sup>	Equilibrium Geometry <sup>a</sup>			Adsorption Energy (kcal/mol)	Vibrational Frequency Normal to Surface (cm <sup>-1</sup> )
	x(a <sub>0</sub> )	y(a <sub>0</sub> )	z(a <sub>0</sub> )		
none	3.12	3.12	1.39	103.7	1219
step	3.23	3.12	1.45	101.5	1128
kink	3.20	3.20	1.50	99.8	1075

<sup>a</sup> The origin was located at a lattice site in the top layer of an unrelaxed lattice. The calculations were performed with the top layer of the surface in its relaxed geometry.

<sup>b</sup> The defects are discussed in Section III.A.

TABLE IX. HYDROGEN ADSORPTION ON SEMI-INFINITE SURFACES OF Cr

Defect <sup>b</sup>	Morse Parameter Set <sup>c</sup>	Equilibrium Geometry <sup>a</sup>			Adsorption Energy (kcal/mol)	Vibrational Frequency Normal to Surface (cm <sup>-1</sup> )
		x(a <sub>0</sub> )	y(a <sub>0</sub> )	z(a <sub>0</sub> )		
none	(1)	2.72	2.72	3.50	74.0	746
	(2)	2.72	2.72	4.50	75.0	996
step	(1)	3.00	2.72	3.59	68.4	736
	(2)	3.03	2.72	4.58	69.5	978
defect	(1)	2.99	2.99	3.67	63.5	728
	(2)	3.02	3.02	4.65	64.8	961

<sup>a</sup> The origin was located at a lattice site in the top layer of an unrelaxed lattice. The calculations were performed with the top layer of the surface in its relaxed geometry.

<sup>b</sup> The defects are discussed in Section III.A.

<sup>c</sup> The parameter set used in these calculations were those given in Table VI.

TABLE X. NITROGEN ADSORPTION ON SEMI-INFINITE SURFACES OF Fe

Defect <sup>b</sup>	Morse Parameter Set <sup>c</sup>	Equilibrium Geometry <sup>a</sup>			Adsorption Energy (kcal/mol)	Vibrational Frequency Normal to Surface (cm <sup>-1</sup> )
		x(a <sub>0</sub> )	y(a <sub>0</sub> )	z(a <sub>0</sub> )		
none	(1)	2.71	2.71	5.03	79.7	279
	(2)	2.71	2.71	3.97	119.7	254
step	(1)	3.14	2.71	5.10	73.6	273
	(2)	3.11	2.71	4.07	109.9	251
kink	(1)	3.12	3.12	5.17	68.1	257
	(2)	3.09	3.09	4.16	101.4	248

<sup>a</sup> The origin was located at a lattice site in the top layer of an unrelaxed lattice. The calculations were performed with the top layer of the surface in its relaxed geometry.

<sup>b</sup> The defects are discussed in Section III.A.

<sup>c</sup> The parameter set used in these calculations were those given in Table VI.

TABLE XI. NITROGEN ADSORPTION ON SEMI-INFINITE SURFACES OF Ta.

Defect <sup>b</sup>	Morse Parameter Set <sup>c</sup>	Equilibrium Geometry <sup>a</sup>			Adsorption Energy (kcal/mol)	Vibrational Frequency Normal to Surface (cm <sup>-1</sup> )
		x(a <sub>0</sub> )	y(a <sub>0</sub> )	z(a <sub>0</sub> )		
none	(1)	3.12	3.12	1.10	140.1	275
	(2)	3.12	3.12	1.39	103.7	327
step	(1)	3.28	3.12	1.14	134.1	257
	(2)	3.23	3.12	1.45	101.5	303
kink	(1)	3.25	3.25	1.18	129.0	244
	(2)	3.20	3.20	1.50	99.8	289

<sup>a</sup> The origin was located at a lattice site in the top layer of an unrelaxed lattice. The calculations were performed with the top layer of the surface in its relaxed geometry.

<sup>b</sup> The defects are discussed in Section III.A.

<sup>c</sup> The parameter set used in these calculations were those given in Table VI.



TABLE XII. NITROGEN ADSORPTION ON SEMI-INFINITE SURFACE OF Cr

Defect <sup>b</sup>	Morse Parameter Set <sup>c</sup>	Equilibrium Geometry <sup>a</sup>			Adsorption Energy (kcal/mol)	Vibrational Frequency Normal to Surface (cm <sup>-1</sup> )
		x(a <sub>0</sub> )	y(a <sub>0</sub> )	z(a <sub>0</sub> )		
none	(1)	2.72	2.72	4.98	89.9	295
	(2)	2.72	2.72	4.00	129.9	266
step	(1)	3.17	2.72	5.08	82.8	289
	(2)	3.17	2.72	4.11	119.0	262
kink	(1)	3.15	3.15	5.15	76.6	283
	(2)	3.14	3.14	4.20	109.7	259

<sup>a</sup> The origin was located at a lattice site in the top layer of an unrelaxed lattice. The calculations were performed with the top layer of the surface in its relaxed geometry.

<sup>b</sup> The defects are discussed in Section III.A.

<sup>c</sup> The parameter set used in these calculations were those given in Table VI.

TABLE XIII. Fe-Fe MORSE POTENTIAL PARAMETERS FOR  
A FINITE CLUSTER OF Fe ATOMS

Defect <sup>a</sup>	Atom in Cluster	$D_{BS}$ (kcal/mol)	$\alpha_{BS} (a_0^{-1})$	$R_{BS} (a_0)$
none	46	10.00	0.736	5.34
step	38	10.03	0.735	5.34
kink	33	10.06	0.735	5.34
adatom-step	34	10.09	0.734	5.34
adatom	26	10.14	0.731	5.35

<sup>a</sup> Defects are discussed in Section III.A.

TABLE XIV. ATOM-ATOM MORSE PARAMETERS FOR HYDROGEN ADSORPTION ON FINITE Fe CLUSTERS<sup>a</sup>

Defects <sup>b</sup>	Atoms in Cluster	Morse Parameters		
		$D_{BS}(\text{kcal/mol})$	$\alpha_{BS}(\text{a}_0^{-1})$	$R_{BS}(\text{a}_0)$
none	30	5.75	0.478	5.86
step	26	5.74	0.481	5.91
kink	23	5.77	0.482	5.91

<sup>a</sup> The Morse parameters were calculated so that the adsorption energies and vibrational frequencies in Table VII were reproduced for a finite cluster.

<sup>b</sup> The defects are discussed in Section III.A.

TABLE XV. ATOM-ATOM MORSE PARAMETERS FOR HYDROGEN ADSORPTION ON FINITE Ta CLUSTERS<sup>a</sup>

Defect <sup>b</sup>	Atoms in Cluster	Morse Parameters		
		$D_{BS}(\text{kcal/mol})$	$\alpha_{BS}(\text{a}_0^{-1})$	$R_{BS}(\text{a}_0)$
none	30	17.14	0.841	4.68
step	26	17.12	0.841	4.68
kink	23	17.11	0.840	4.68

<sup>a</sup> The Morse parameters were calculated so that the adsorption energies and vibrational frequencies in Table VIII were reproduced for a finite cluster.

<sup>b</sup> The defects are discussed in Section III.A.

TABLE XVI. ATOM-ATOM MORSE PARAMETER FOR HYDROGEN ADSORPTION ON FINITE Cr CLUSTERS<sup>a</sup>

Defects <sup>b</sup>	Atom in Cluster	Morse Parameter Set <sup>c</sup>	Morse Parameter		
			$D_{BS}(\text{kcal/mol})$	$\alpha_{BS}(\text{a}_0^{-1})$	$R_{BS}(\text{a}_0)$
none	30	(1)	6.44	0.486	5.86
		(2)	7.70	0.559	6.31
step	26	(1)	6.47	0.484	5.82
		(2)	7.71	0.557	6.28
kink	23	(1)	6.49	0.483	5.79
		(2)	7.73	0.555	6.2

<sup>a</sup> The Morse parameters were calculated so that the adsorption energies and vibrational frequencies in Table XI were reproduced for a finite cluster.

<sup>b</sup> The defects are discussed in Section III.A.

<sup>c</sup> The parameters sets correspond to those used in Table VI.

TABLE XVII. ATOM-ATOM MORSE PARAMETERS FOR NITROGEN ADSORPTION ON FINITE Fe CLUSTERS<sup>a</sup>

Defects <sup>b</sup>	Atom in Cluster	Morse Parameter Set <sup>c</sup>	Morse Parameter		
			$D_{BS}(\text{kcal/mol})$	$\alpha_{BS}(a_0^{-1})$	$R_{BS}(a_0)$
none	30	(1)	7.92	0.545	6.64
		(2)	9.79	0.461	6.16
step	26	(1)	7.96	0.544	6.60
		(2)	9.87	0.460	6.12
kink	23	(1)	7.98	0.544	6.60
		(2)	9.93	0.460	6.11

<sup>a</sup> The Morse parameters were calculated so that the adsorption energies and vibrational frequencies in Table X were reproduced for a finite cluster.

<sup>b</sup> The defects are discussed in Section III.A.

<sup>c</sup> The parameters sets correspond to those used in Table VI.

TABLE XVIII. ATOM-ATOM MORSE PARAMETERS FOR NITROGEN ADSORPTION  
ON FINITE Ta CLUSTERS<sup>a</sup>

Defects <sup>b</sup>	Atom in Cluster	Morse Parameter Set <sup>c</sup>	Morse Parameter		
			$D_{BS}(\text{kcal/mol})$	$\alpha_{BS}(\text{a}_0^{-1})$	$R_{BS}(\text{a}_0)$
none	30	(1)	16.76	0.579	4.89
		(2)	17.14	0.841	4.68
step	26	(1)	16.66	0.577	4.89
		(2)	17.12	0.841	4.68
kink	23	(1)	16.59	0.576	4.90
		(2)	17.11	0.840	4.68

<sup>a</sup> The Morse parameters were calculated so that the adsorption energies and vibrational frequencies in Table XI were reproduced for a finite cluster.

<sup>b</sup> The defects are discussed in Section III.A.

<sup>c</sup> The parameters sets correspond to those used in Table VI.

TABLE XIX. ATOM-ATOM MORSE PARAMETERS IN NITROGEN ADSORPTION  
ON FINITE Cr CLUSTERS<sup>a</sup>

Defects <sup>b</sup>	Atom in Cluster	Morse Parameter Set <sup>c</sup>	Morse Parameter		
			$D_{BS}(\text{kcal/mol})$	$\alpha_{BS}(a_0^{-1})$	$R_{BS}(a_0)$
none	30	(1)	8.68	0.539	6.73
		(2)	10.26	0.453	6.30
step	26	(1)	8.72	0.538	6.70
		(2)	10.31	0.451	6.26
kink	23	(1)	8.72	0.536	6.68
		(2)	10.39	0.451	6.239

<sup>a</sup> The Morse parameters were calculated so that the adsorption energies and vibrational frequencies in Table XII were reproduced for a finite cluster.

<sup>b</sup> The defects are discussed in Section III.A.

<sup>c</sup> The parameters sets correspond to those used in Table VI.

# XX. ENERGETICS OF ATOMIC RECOMBINATION ON METAL SURFACES

Diatomic	Metal	Morse Parameter Set <sup>a</sup>	Defect <sup>b</sup>	Atomic Adsorption Energy (kcal/mol)	Diatomic Dissociation Energy <sup>c</sup> (kcal/mol)	$\Delta E_R^c$ (kcal/mol)
H <sub>2</sub>	Fe		none	66.7	109.5	42.8
			step	61.0	109.5	48.5
			kink	56.4	109.5	53.1
N <sub>2</sub>	Fe	(1)	none	79.7	228.4	148.7
			step	73.6	228.4	154.8
			kink	68.1	228.4	160.3
N <sub>2</sub>	Fe	(2)	none	119.7	228.4	108.7
N <sub>2</sub>	Ta	(1)	none	103.7	228.4	124.7
			step	101.5	228.4	126.9

<sup>a</sup> The Morse parameter sets are those given in Table XI.

<sup>b</sup> Defects are discussed in Section III.A.

<sup>c</sup> Exoergicity for the Rideal process.



TABLE XXI. TRAJECTORY RESULTS FOR ATOM RECOMBINATION ON METAL SURFACES BY A RADEAL MECHANISM<sup>a</sup>

System	Morse Parameter Set <sup>b</sup>	Defect <sup>c</sup>	$E_T^d$ (kcal/mol)	$T_S^e$ (K)	$P_R^f$	$\Delta E_S^g$ (kcal/mol)	$\Delta E_S/\Delta E_R^h$ (kcal/mol)
H <sub>2</sub> on Fe		none	2.31	1500	.04	15	.3
			4.62	1500	.02	5	.1
			6.93	1500	.03	10	.2
N <sub>2</sub> on Fe	(1)	none	2.31	1500	.70	39	.27
			4.62	1000	.71	38	.26
			4.62	1500	.62	37	.26
			4.62	2000	.62	38	.26
			4.62	2500	.44	48	.33
			9.24	1500	.78	42	.28
			4.62	1500	.65	38	.25
			9.24	1500	.55	40	.26
N <sub>2</sub> on Fe	(2)	kink	4.62	1500	.65	38	.24
			9.24	1500	.53	39	.25
			4.62	1500	.07	51	.5
			9.24	1500	.02	50	.5
N <sub>2</sub> on Ta	(1)	none	2.31	1500	.91	10	.09
			4.62	1500	.90	9	.08
			4.62	2000	.86	12	.10
			4.62	2500	.85	10	.09
			9.24	1500	.95	6	.05
			9.24	2000	.86	14	.11
			9.24	2500	.84	13	.11
			4.62	1500	.94	14	.11
			6.93	1500	.89	10	.08
			9.24	1500	.90	12	.10

- a All results presented here are for trajectories with normal incidence to the surface.
- b Morse parameter sets are those given in Table XVII and XVIII.
- c Defects are discussed in Section III.A.
- d Incident translation energy.
- e Temperature of surface.
- f Probability for a direct recombination reaction (i.e., no long lived adsorbed complexes).
- g Energy transfer to surface in atom-recombination reactions.
- h Fraction of exocigicity deposited into the surface.

TABLE XXII. RESULTS OF TRAJECTORY CALCULATIONS FOR NITROGEN ATOM RECOMBINATION ON Fe SURFACES FOR NON-NORMAL INCIDENCE OF THE GAS ATOM<sup>a</sup>

Defect	$E_T$ (kcal/mol)	$\theta$	$\phi$	$P_R$	$\Delta E_S$ (kcal/mol)	$\Delta E_S/\Delta E_R$
none	9.24	30°	180°	.63	46	.31
	9.24	30°	150°	.85	57	.39
step	4.62	30°	180°	.89	45	.29
kink	4.62	30°	180°	.92	51	.32

<sup>a</sup> All trajectories are for Morse parameter set (1) and a surface temperature of 1500K.

APPENDIX A

## MODEL POTENTIAL FOR THE INTERACTION OF MOLECULES WITH AMORPHOUS SURFACES \*

George D. PURVIS III and George WOLKEN Jr.  
*Battelle, Columbus Laboratories, Columbus, Ohio 43201, USA*

Received 30 October 1978

Previous models for gas-surface interactions have utilized either pairwise forces or semi-empirical potentials formulated in terms of perfect two-dimensional surfaces. Here, we combine the pairwise model with existing semi-empirical models, retaining the realistic chemical forces of the semi-empirical model, but having direct applicability to surfaces with non-periodic structures.

### 1. Introduction

In a previous paper [1], we presented a model potential that has the appropriate characteristics for describing the reactions of diatomic molecules with solid surfaces. One of the primary objectives of this line of research has been to model in a realistic way the dynamics of chemical reactions occurring on and with solid surfaces. For this end, a model potential must have three properties: (1) It must be realistic, reproducing the experimental binding energies, activation barriers, etc., so far as they are known; (2) it must be flexible, capable of modelling a variety of different potentials by the same overall procedure; and (3) it must be tractable, such that forces experienced by each atom can be rapidly computed and classical trajectory studies can be performed. The London-Eyring-Polanyi-Sato (LEPS) [2] seemed to meet these three criteria and has been used as the starting point for a variety of studies of heterogeneous reaction dynamics [3]. While the original LEPS model treated the solid surface as rigid [2], it was soon generalized to permit oscillations of the surface atoms [4], generalized Langevin oscillators [5], and reactions with the solid itself [1]. However, the model potential as implemented thus far has only been used for surfaces with perfect two-dimensional symmetry (apart from local oscillations

or displacement from equilibrium lattice positions). In this note, we point out that the LEPS potential can be re-formulated in such a way that imperfect crystals can be modelled keeping the same realism, flexibility, and tractability that has been so useful in these recent studies. There is considerable evidence that many catalytic reactions proceed on steps [6] and amorphous metals have many interesting surface chemical properties [7]. Therefore, it is important to add ways to study such systems to our arsenal of computational procedures.

In this note, we alter the modified LEPS potential function to allow the treatment of non-rigid surfaces with arbitrary geometries. This could include genuinely amorphous materials, polycrystalline samples with steps, kinks, etc. The alteration is straightforward. Previously [2] the interaction of one gas atom with the solid surface was assumed to be a Morse function in the direction perpendicular to the surface. The Morse parameters were allowed to be periodic functions of the  $X$  and  $Y$  distances over the surface. The values of the parameters were fixed to those values which gave agreement with known experimental or theoretical values for binding energies of the fragment to the surface. We call this potential  $Q_{\text{periodic},A}$  understanding that it describes the interaction of a single atom ( $A$ ) with a solid surface, periodic in  $X, Y$ . The final LEPS model was given as a functional of  $Q_{\text{periodic},A}$  and the potential describing the interaction of the two gas atoms  $V_{A,B}$ . Therefore, the LEPS formulation for the

\* This research was sponsored by the U.S. Army Research Office under Contract Number DAAG29-77-0047.

periodic surface is

$$V_{\text{periodic}} = F\{Q_{\text{periodic},A}; Q_{\text{periodic},B}; V_{A,B}\}. \quad (1)$$

Correction terms have been added onto this basic model potential to allow for motion of the surface atoms, erosion, etc., but they are not essential to our present discussion.

The present modification replaces  $Q_{\text{periodic}}$  with a sum of pairwise forces between the gas atoms and each surface atom, but retains the functional dependence in eq. (1). That is, if  $S$  denotes the set of atoms in the solid, the usual pairwise model for atom-surface interactions is simply

$$Q_{\text{pairwise},A} = \sum_{i \in S} q_{iA}, \quad (2)$$

where  $q_{iA}$  is the two-body force between solid atom  $i$  and gas atom  $A$ . A fully pairwise description of the interaction between diatomic molecule  $AB$  and the solid is then

$$V_{\text{pairwise}} = Q_{\text{pairwise},A} + Q_{\text{pairwise},B} + V_{A,B}. \quad (3)$$

As discussed elsewhere [1], this is not expected to be satisfactory for many cases of interest. However, the modification proposed here is simply to use  $Q_{\text{pairwise}}$  in eq. (1) in place of  $Q_{\text{periodic}}$  giving

$$V_{\text{amorphous}} = F\{Q_{\text{pairwise},A}; Q_{\text{pairwise},B}; V_{A,B}\}. \quad (4)$$

Thus the entire LEPS formulation given previously follows through changing simply the form of the underlying component interactions. The form of the potential for diatomic  $AB$  on surface  $S$  is

$$V_{\text{LEPS}} = U_{AB} + U_{AS} + U_{BS} - [A_{AB}^2 + (A_{AS} + A_{BS})^2 - A_{AB}(A_{AS} + A_{BS})]^{1/2}, \quad (5)$$

where

$$U_{AB} = \frac{D_{AB}}{4(1 + \Delta_{AB})} \{ (3 + \Delta_{AB}) \exp[-2\alpha_{AB}(r_{AB} - R_{AB})] - (2 + 6\Delta_{AB}) \exp[-\alpha_{AB}(r_{AB} - R_{AB})] \}, \quad (6)$$

$$A_{AB} = \frac{D_{AB}}{4(1 + \Delta_{AB})} \{ (1 + 3\Delta_{AB}) \exp[-2\alpha_{AB}(r_{AB} - R_{AB})] - (5 + 2\Delta_{AB}) \exp[-\alpha_{AB}(r_{AB} - R_{AB})] \}, \quad (7)$$

$$U_{AS} = \frac{1}{4(1 + \Delta_{AS})} \sum_{i \in S} D_{Ai} \times \{ (3 + \Delta_{AS}) \exp[-2\alpha_{Ai}(r_{Ai} - R_{Ai})] - (2 + 6\Delta_{AS}) \exp[-\alpha_{Ai}(r_{Ai} - R_{Ai})] \}, \quad (8)$$

$$A_{AS} = \frac{1}{4(1 + \Delta_{AS})} \sum_{i \in S} D_{Ai} \times \{ (1 + 3\Delta_{AS}) \exp[-2\alpha_{Ai}(r_{Ai} - R_{Ai})] - (6 + 2\Delta_{AS}) \exp[-\alpha_{Ai}(r_{Ai} - R_{Ai})] \}, \quad (9)$$

and  $D_{PQ}$ ,  $\alpha_{PQ}$ , and  $R_{PQ}$  are the dissociation energy, Morse parameter and equilibrium distance for the two-body interaction between  $P$  and  $Q$ .  $U_{BS}$  and  $A_{BS}$  are derived from eqs. (8) and (9) by substituting  $B$  for  $A$ .  $\Delta_{PQ}$  is the Sato parameter used to generate a variety of surfaces. Only a change in the expressions for the two-body atom-surface Coulomb and exchange integrals has been required. The use of the pairwise additive atom-solid potential as a single two-body potential is consistent with the requirement (imposed during the derivation of the modified LEPS potential) [2] that the surface acts as an extended source of one and two electrons, as required, for bonding the incident fragments.

In fig. 1 we compare the periodic potential from ref. [1] (fig. 3b) for  $H_2$  interacting with the (001) face of iron with  $V_{\text{amorphous}}$  obtained from considering the interaction with a cluster of 33 Fe atoms (fig. 2). The pairwise forces  $q_{iA}$  in eq. (2) have the form of Morse potentials

$$q_{iA} = D_0 \exp[-(m/r_0)(r_{iA} - r_0)] \times \{ \exp[-(m/r_0)(r_{iA} - r_0)] - 2 \}, \quad (10)$$

where  $D_0 = 4.6$  kcal,  $r_0 = 3.11$  Å,  $m = 2.96$ . We see in fig. 1 that the potentials have some differences quantitatively, but have the same qualitative structure. That is, there is an activation barrier to adsorption approximately in agreement with experiment [1,8] and no molecular adsorption is present. For large H-H separations, when both atoms lie on the surface, there are some effects from the finite size of the cluster and the neglect of continuum contributions [9]. Also, the  $H_2$ -Fe interaction more rapidly decreases for the cluster than for the infinite surface as  $H_2$  recedes from the surface.

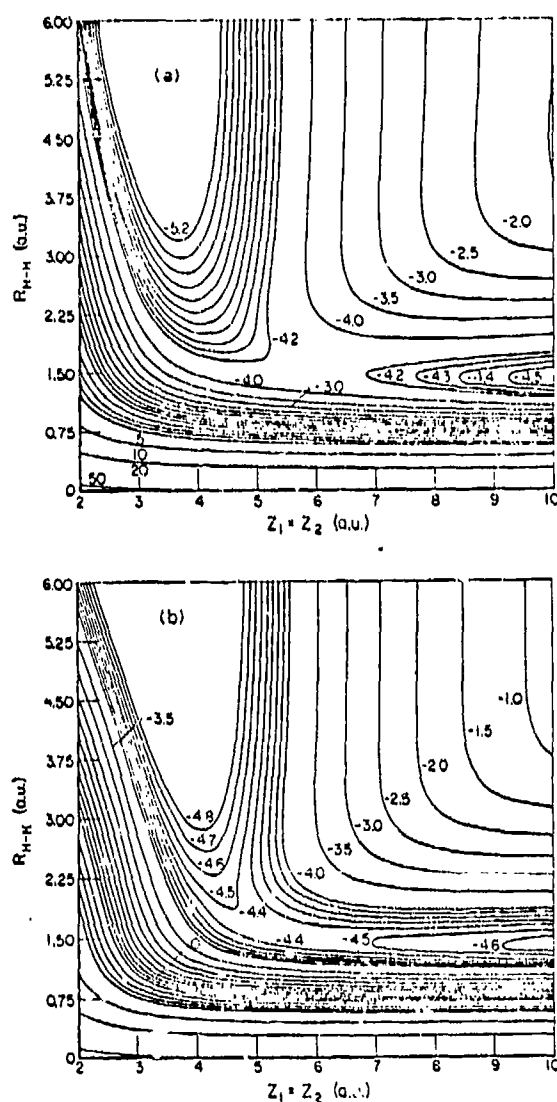


Fig. 1. Equipotential contours (in eV) for the approach of H<sub>2</sub> towards the iron surface. The H-H bond is parallel to the surface, the bond midpoint is centered over a 1CN site, and oriented in the direction of adjoining 5CN sites (defined in fig. 2). This path leads to the smallest barriers to adsorption as well as the most tightly bound adsorbed atoms. (a)  $V_{\text{periodic}}$  from eq. (1); (b)  $V_{\text{amorphous}}$  from eq. (4).

However, at present there is no way to determine from experiment which fit is preferable, so we forgo extensive variation of parameters to produce a fully adjusted surface.

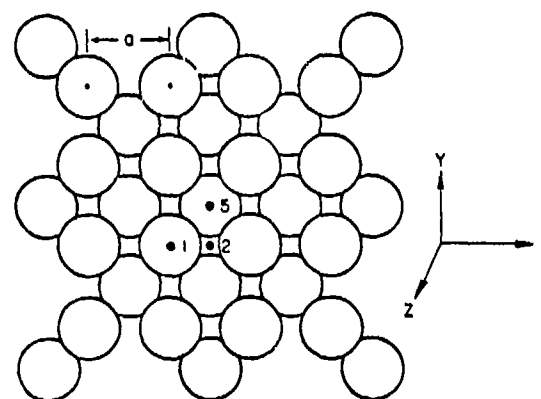


Fig. 2. Thirty-three atom cluster representing the (001) face of bcc Fe. An adsorbed atom at sites 1, 2, and 5 would be coordinated to one, two, or five iron atoms, respectively. The positive Z axis is directed away from the surface and the origin of coordinates is at the lattice site beneath a singly coordinated (1CN) site,  $a = 5.42$  au.

The parameters used in eq. (10) are precisely those used by Olander in his model of H-Fe(001) [9].  $V_{\text{pairwise}}$  is shown in fig. 3, produced from eq. (3) using these potentials. As discussed in ref. [1], molecular adsorption is not observed for H<sub>2</sub> + Fe(001) and is a distinct inadequacy of the pairwise model.

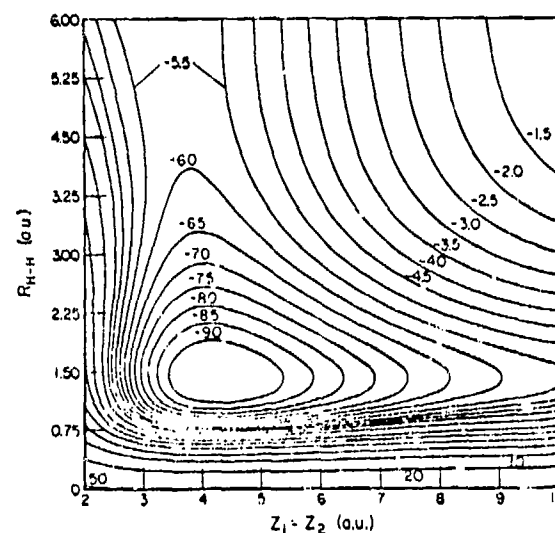


Fig. 3. Interaction generated from  $V_{\text{pairwise}}$  using eq. (3). The other conditions are the same as fig. 1.

In conclusion, the substitution of a pairwise additive fragment-surface interaction potential for the previously-used periodic potential seems to yield a useful potential function for the study of gas-amorphous surface interactions. It retains most of the flexibility of the previous model while providing correct functional forms for several new cases of interest including amorphous solid structures, energy transfer to the surface, and erosion.

#### References

- [1] G. Wolken Jr., J. Chem. Phys. 68 (1978) 4338.
- [2] J.H. McCreery and G. Wolken Jr., J. Chem. Phys. 63 (1975) 2340.
- [3] A.R. Gregory, A. Gelb and R. Silby, Surface Sci. 74 (1978) 497;  
G.D. Purvis, M.J. Redmon and G. Wolken Jr., J. Phys. Chem., submitted for publication.
- [4] J.H. McCreery and G. Wolken Jr., J. Chem. Phys. 67 (1977) 2551.
- [5] A.C. Diebold and G. Wolken Jr., Surface Sci. 82 (1979) 245.
- [6] D. Brennan, Progr. Surface Sci. 2 (1964) 57.
- [7] F. Chaudhari and D. Turnbull, Science 199 (1978) 11.
- [8] R.A. Oriani, Ber. Bunsenges. Physik. Chem. 76 (1972) 848.
- [9] D.R. Olander, J. Phys. Chem. Solids 32 (1971) 7499.